# Friedel Oscillations are Limiting the Strength of Superhard Nanocomposites and Heterostructures

R. F. Zhang,[1] A. S. Argon,[2] and S. Veprek[1,*]

[1]*Department of Chemistry, Technical University Munich, Lichtenbergstrasse 4, D-85747 Garching, Germany*
[2]*Department of Mechanical Engineering, Massachusetts Institute of Technology,
77 Massachusetts Avenue, Cambridge, Massachusetts 02139, USA*

To obtain a deeper understanding of the mechanism of plastic deformation and failure in superhard nanocomposites and heterostructures we studied, by means of the *ab initio* density functional theory, the stress-strain response and the change of the electronic structure during tensile and shear deformation of a prototype interfacial systems consisting of 1 monolayer SiN sandwiched between a few nm thick TiN layers. This shows that peak Friedel oscillations of valence charge density weaken the Ti-N interplanar bonds next to that interface, where decohesion in tension and slip in shear occurs. These results provide ways to design new, stronger and harder materials.

Superhard nanocomposites consisting of 3–4 nm size, randomly oriented [1] nanocrystals of stable, hard transition metal nitride (TmN) "glued" together by about one monolayer (1 ML) of a covalent nitride (e.g., $Si_3N_4$), with hardness between 45 [2] to $\geq 100$ GPa [3] have attracted wide attention of the scientific community, and have already found large-scale industrial applications [4]. Hardness maxima of 33 to 35 GPa have recently been reported also for fcc-TmN/SiN/TmN heterostructures when the pseudomorphic fcc-SiN, between roughly 4 nm thick TiN [5–10] or ZrN [11] slabs, was about 1 to 2 ML thick. Because the TiN-$SiN_x$ system is regarded as a "prototype" of all nitride-based superhard nanocomposites, we focus on it in this Letter.

Hao *et al.* studied the stoichiometric TiN-$Si_3N_4$ system by means of *ab initio* density functional theory (DFT). They found that the strongest configuration is a TiN/$Si_3N_4$/TiN sandwich containing 1 ML of $\alpha$- or $\beta$-$Si_3N_4$-derived interfaces possessing decohesion strength larger than that of bulk $Si_3N_4$ [12]. They also confirmed [13] the experimental finding [14] that oxygen impurities strongly degrade the strength of the $Si_3N_4$ interface. Liu *et al.* studied several configurations of Si-atoms incorporated into TiN and found that the highest cohesive energy of 426.86 eV (bulk Ti-N 430.19 eV) have Si atoms tetrahedrally coordinated to 4N and 4Ti atoms with Si-N bonds being significantly shorter than the Si-Ti distance [15].

We have shown that 1 ML of the interfacial, substoichiometric, pseudomorphic SiN is strengthened by a factor of 4 to 10 [16] as compared with bulk SiN [17]. Using the shear strength of the TiN/1 ML-SiN/TiN interfaces, calculated by *ab initio* DFT, Sachs averaging of these to obtain a tensile yield strength of the nanocrystalline assembly of grains, together with appropriately accounting for pressure enhancement of the shear resistances of the interfaces and using the Tabor relationship between hardness and the

yield strength, the measured superhardness in excess of 100 GPa of nanocomposites has been fully explained [16]. However, in the papers quoted here, the electronic structure of the interface and its effect on the mechanism of decohesion and ideal shear under applied stress had not been studied. This is the subject of the present Letter which reveals for the first time that, although SiN is the weakest of all covalent materials under consideration, and unstable in bulk, the weakest link in the TiN/1 ML-SiN/TiN sandwich is the bond between Ti and N atoms within the interlayer next to the $SiN_x$ interface. This is a consequence of the ubiquitous Friedel oscillations that are found in electronically perturbed solids adjacent to their surfaces and interfaces [18].

The *ab initio* DFT calculations were done using the "Vienna *ab initio* simulation package" (VASP) [19] with the projector augmented wave method employed to describe the electron-ion interaction [20], and the generalized-gradient approximation of Perdew and Wang (PW91) [21] for the exchange-correlation term together with the Vosko-Wilk-Nusair interpolation. The integration in the Brillouin zone has been done on special $k$ points of $5 \times 5 \times 3$ grids for the interface systems, determined according to the Monkhorst-Pack scheme, energy cutoff of 600 eV, and the tetrahedron method with Blöchl corrections for the charge density calculation, and Gaussian smearing for the stress calculations. The conjugate gradient method has been used for the relaxation of structural parameters. The stress-strain relationships were calculated by incrementally deforming the modeled cell in the direction of the applied strain, and simultaneously relaxing both the simulation cell basis vectors as well as the positions of atoms inside the unit cell, at each step. To ensure that the strain path is continuous, the starting position at each strain step has been taken from the relaxed coordinates of the previous strain step. We have also checked the convergence

by calculating the stress-strain curves for $7 \times 7 \times 5$ $k$-points and found no significant difference beyond a few percent. The extensive checks of the reliability of our calculations can be found in our earlier papers [16,17,22].

The next step has been to verify the stability of the chosen (111), (110), and (100) interfaces because some of the stress-strain curves for bulk SiN in our earlier paper showed a concave shape at small strains (see Fig. 2 in Ref. [17]), which is a hint that there is a local maximum of the total energy at zero strain; i.e., the symmetric, undistorted fcc-SiN is inherently instable. This is not surprising because there are many examples where a highly symmetric configuration in crystals or molecules decreases their energy by decreasing their symmetry (e.g., Jahn-Teller distortion, lowering of symmetry to a noncentric space group in ferroelectrics below the Curie temperature, the split interstitial effect in fcc metals, inert pair effect, and the like [23]). To verify the stability of the 1ML-SiN interfaces between the TiN slabs, we first relaxed the original structure as described in [16] to a minimum of the total energy which resulted in certain changes of the original configuration (cf. Figs. 4 and 5 in [16]). Afterwards, we applied small distortions to the interfacial Si atoms in the chosen crystallographic directions $x$, $y$, $xy$, and $z$, where $x$ and $y$ are Cartesian coordinates within the plane of the SiN interface and $z$ is perpendicular to it. As a result we found that (111) and (110) interfaces are (locally) stable because the total energy increased upon a distortion of 1% to 3%, whereas the (100) interface is unstable because the total energy decreased. The (111) interface possesses the highest symmetry of a tetragonally distorted octahedron with Si-N bonds slightly elongated in the $z$ direction, whereas the (110) interface shows a distortion also within the $x$-$y$ plane. In contrast, the total energy of the (100) interface decreased with a small distortion, but it reached a minimum at a distortion of about 12%. This distorted state is (locally) stable [24]. In this letter, we focus on the (111) interface in order to show the general effect of Friedel oscillations on the mechanism of decohesion and ideal shear. The (111) interface is a representative example for all other interfaces although details of the symmetry changes and quantitative values are more complex [24].

Figure 1 shows the cell with the (111) 1 ML-SiN interface after relaxation to minimum total energy, with the interatomic bond distances [Fig. 1(a)] and the valence charge density (VCD) [Fig. 1(b)]. The Si-N bond length of 0.1993 nm is shorter than that in bulk SiN (0.2131 nm) reflecting the strengthening of the SiN interface. However, the length of the Ti-N bonds of 0.2324 nm next to the SiN interface is the largest of all other Ti-N bonds which show damped oscillations moving away from the interface. These oscillations of bond lengths in Fig. 1(a) are representative of Friedel oscillations [18] of the valence charge density shown in Fig. 1(b). They reflect the strengthening
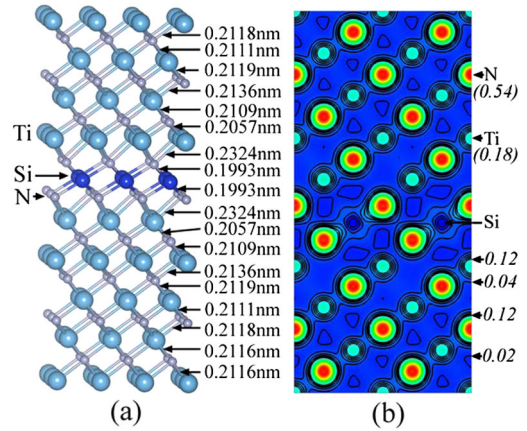


FIG. 1 (color online).   Perspective view of the relaxed (111) 1 ML-SiN interface showing in Fig. 1(a) the damped oscillations of the bond lengths which reflect the Friedel oscillations of valence charge density in Fig. 1(b). The valence charge density (VCD) scales from 0 (dark blue) to 0.54 electrons/Bohr³ (bright red), and the italic numbers indicate the charge values of several VCD contours.

of the covalent Si-N bonds and the significant weakening of the neighbor Ti-N bonds.

Now we show that the weakest links are not the Si-N bonds within the SiN interface, but the Ti-N interplanar bonds within the TiN nanocrystal between the first and second Ti-N planes from the SiN interface, which has the longest Ti-N bonds of 0.2324 nm, and where decohesion and shear occur. Figure 2 shows the calculated stress-strain curves for tensile loading in a direction perpendicular to the interface and for two relevant slip systems in shear as indicated in the inset. Figure 3 shows the VCD under tensile stress just before the instability [Fig. 3(a)] corresponding to the peak on the tensile stress-strain curve in
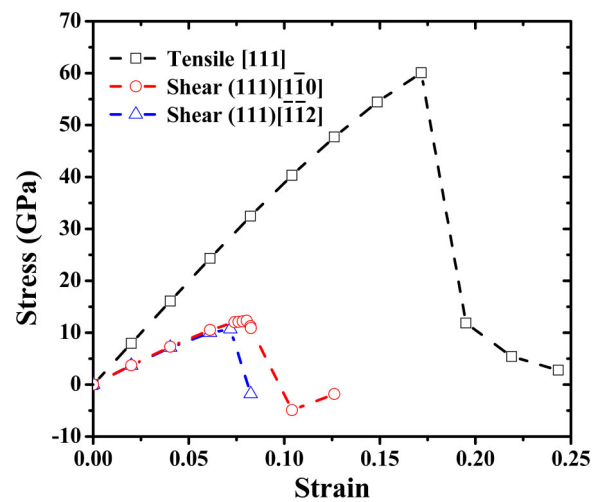


FIG. 2 (color online).   Calculated stress-strain curves of the (111) interface in tension applied to the model cell in a direction perpendicular to the interface and for shear in the slip systems as indicated in the inset.
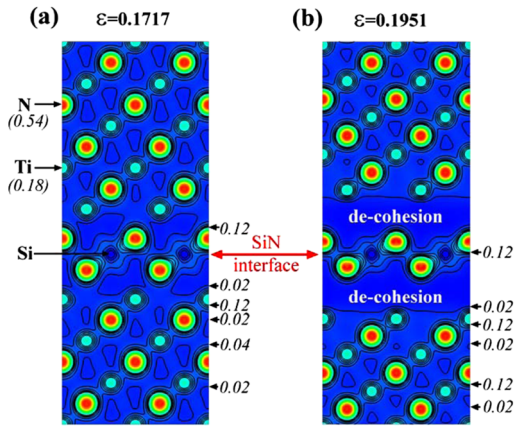
FIG. 3 (color online).   Changes of the valence charge density under an applied tensile strain normal to the (111) interface just before the instability (a) and just after it (b). The strains $\varepsilon$ allow the reader to identify the corresponding points on the tensile stress-strain curve in Fig. 2. The valence charge density scales range from 0 (dark blue) to 0.54 electrons/Bohr$^3$ (bright red).



FIG. 4 (color online).   Valence charge density of the (111) interface under applied shear stress in the $[1\bar{1}0]$ direction just before [(a); strain $\gamma = 0.0824$] and after [(b); strain $\gamma = 0.1041$] the shear instability. The white arrow shows the flipover of the Ti-N bond from atom Ti(1) to Ti(2) due to the shear. (c) The top view, normal to the (111) interface, showing the relative initial atomic movement in shear, and the viewing direction of the structure in (a) and (b). The valence charge density scales range from 0 (dark blue) to 0.54 electrons/Bohr$^3$ (bright red).

Fig. 2 and just after it [Fig. 3(b)]. It is seen that decohesion occurs between the nitrogen atoms within the SiN interfacial layer and Ti atoms next to it, i.e., within the interplanar gap with the largest spacing [Fig. 1(a)]. Decohesion is important for understanding brittle fracture, whereas plastic deformation occurs in shear under constant volume (compatibility conditions). Therefore, we show in Fig. 4 the VCD for the (111)$[1\bar{1}0]$ slip system just before, (a) and (b) after the ideal shear instability. The values of the shear strain given in the figures identify the corresponding points on the stress-strain curve in Fig. 2. The arrows show the flipover of the Ti-N bond from N-atom number 1 to N-atom number 2 upon the shear instability event. Obviously, the ideal shear occurs between the Ti-N interplanar bonds with the largest bond distance. Figure 4(c) shows the direction of the initial atomic movement in this slip step. Interestingly, the atomic slip step does not occur in the $[1\bar{1}0]$ direction of the applied shear stress, but within the (111) plane along the $[1\bar{2}1]$ direction as indicated by the dashed (red) arrow. Under continued shear flow, the atomic movements will occur in a zigzag manner by two complementary $[1\bar{2}1]$ and $[2\bar{1}\,\bar{1}]$ steps, resulting in an overall shear movement in the $[1\bar{1}0]$ direction of the applied stress. This kind of shear by two complementary $\langle 121 \rangle$ type partial steps is well known in close packed metals [25], and was first related to the potential energy topography of the {111} planes by Vitek [26], and is now widely used (e.g., [27]). This means that the shear translations of the atoms on the interface are along the energetically most favorable path. Also in the (111)$[\bar{1}\,\bar{1}2]$ slip system (see Fig. 2), shear occurs within the Ti-N interplane bonds with the largest bond distance and lowest valence charge density.

A comparison of the (111) interface with others [16] demonstrates that this interface is the weakest of all. This conclusion remains valid even when the distorted, minimum total energy (100) interface is included in the com-
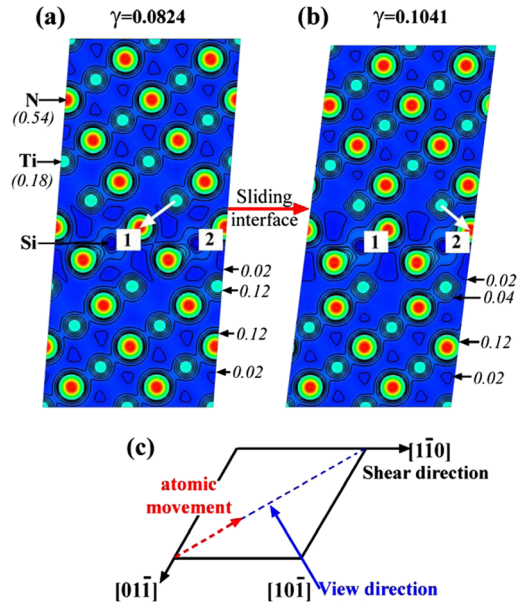
parison [24]. Although some of the decohesion and shear across other interfaces and along other slip systems differs slightly in detail from those shown here for the (111) interface, the overall picture is the same: due to the Friedel oscillations, which are found in solids electronically disturbed by interfaces [18], the weakest link in the fcc-TiN/1 ML-SiN/TiN system studied in the present Letter is the Ti-N interplanar layer next to the strong SiN interface. Our ongoing work shows that also for the (100) and (110) interfaces in this system, as well as in other TmN/1 ML-SiN/TmN systems, the weakest link is either the second or even third Tm-N layer remote from the SiN interface. This applies also to the TiN/Si$_3$N$_4$ interfaces investigated by Hao *et al.*, where interfaces also produced Friedel oscillations [28]. The shortening of the Si-N bonds and elongation of the Ti-Si distances in the "double tetraheder" studied by Liu *et al.* [15] strongly suggest the presence of Friedel oscillations in this case as well. In the superhard nanocomposites with randomly oriented nanocrystals of a regular polyhedral shape [29], a variety of interfaces has to coexist. Our results show that the enhanced strength of the interfaces is still limited by the general appearance of Friedel oscillations adjacent to interfaces.

Because the 3–4 nm size nanocrystals of a strong transition metal nitride, such as TiN studied here, are free of defects and dislocation activity is absent [30], they deform

only elastically. Therefore, the interfaces are the sole carriers of plastic flow [16]. Our recent calculations have shown that already with the relatively weak, thermodynamically unstable SiN interface, hardness of the nanocomposites in excess of 100 GPa can be achieved if the concentration of impurities is sufficiently low [16]. The present results pose an important question worthy of further studies, whether by an appropriate choice of another TmN and covalent nitride ($Si_3N_4$, BN, AlN, …) the Friedel oscillations could be reduced, and an even stronger interface could be obtained.

In conclusion, we have shown that Friedel oscillations of the valence charge density within TiN adjacent to the strong $SiN_x$ interface limit the achievable strength of the $TiN/SiN_x$ interface by weakening the Ti-N interplanar bond strength between the strengthened SiN interface and the TiN layer adjacent to it, and thus are also limiting the achievable strength and hardness of superhard nanocomposites and heterostructures. This phenomenon occurs also at other $TiN/SiN_x$ interfaces and other nc-$TmN$/a-$XN_x$ ($X$ = Si, B, Al, …) and possibly also in related carbide and oxide systems. Therefore, a search for other systems, in which the Friedel oscillations may be diminished, is an appealing task that may help to develop new superhard nanocomposite and heterostructures with an even higher hardness and stability. Compared to hetereostructures, the advantage of the nanocomposites with randomly oriented nanocrystals is the fact that all interfaces, i.e., also the strongest ones, must shear and restructure [16] in order to meet the compatibility requirements. In view of the large-scale industrial applications of the superhard nanocomposites, such studies will be highly demanding, but also potentially very rewarding.

---

*Corresponding author.
veprek@ch.tum.de

[1] A. Niederhofer, P. Nesladek, H.-D. Männling, K. Moto, S. Veprek, and M. Jilek, Surf. Coat. Technol. **120–121**, 173 (1999).

[2] S. Veprek and S. Reiprich, Thin Solid Films **268**, 64 (1995).

[3] S. Veprek, M. G. J. Veprek-Heijman, P. Karvankova, and J. Prochazka, Thin Solid Films **476**, 1 (2005).

[4] S. Veprek and M. G. J. Veprek-Heijman, Surf. Coat. Technol. **202**, 5063 (2008).

[5] H. Söderberg, M. Odén, J. M. Molina-Aldareguia, and L. Hultman, J. Appl. Phys. **97**, 114327 (2005).

[6] X. P. Hu, H. J. Zhang, J. W. Dai, G. Y. Li, and M. Y. Gu, J. Vac. Sci. Technol. A **23**, 114 (2005).

[7] H. Söderberg, M. Odén, T. Larsson, L. Hultman, and J. M. Molina-Aldareguia, Appl. Phys. Lett. **88**, 191902 (2006).

[8] H. Söderberg, M. Oden, A. Flink, J. Birch, P. O. A. Persson, M. Beckers, and L. Hultman, J. Mater. Res. **22**, 3255 (2007).

[9] L. Hultman, J. Bareno, A. Flink, H. Söderberg, K. Larsson, V. Petrova, M. Oden, J. E. Greene, and I. Petrov, Phys. Rev. B **75**, 155437 (2007).

[10] M. Kong, W. J. Zhao, L. Wei, and G. Y. Li, J. Phys. D **40**, 2858 (2007).

[11] Y. S. Dong, W. J. Zhao, J. L. Yue, and G. Y. Li, Appl. Phys. Lett. **89**, 121916 (2006).

[12] S. Hao, B. Delley, and C. Stampfl, Phys. Rev. B **74**, 035402 (2006).

[13] S. Hao, B. Delley, and C. Stampfl, Phys. Rev. B **74**, 035424 (2006).

[14] S. Veprek, P. Karvankova, and M. G. J. Veprek-Heijman, J. Vac. Sci. Technol. B **23**, L17 (2005).

[15] X. J. Liu, B. Gottwald, C. Q. Wang, Y. Jia, and E. Westkämper, *High Performance Computing in Science and Engineering '07*, edited by W. E. Nagel (Springer, Berlin-Heidelberg 2008), p. 117.

[16] S. Veprek, A. S. Argon, and R. F. Zhang, Philos. Mag. Lett. **87**, 955 (2007).

[17] R. F. Zhang, S. H. Sheng, and S. Veprek, Appl. Phys. Lett. **90**, 191903 (2007).

[18] J. Friedel, Philos. Mag. **43**, 153 (1952); W. A. Harrison, *Electronic Structure and Properties of Solids* (W. H. Freeman and Co., San Francisco, 1980).

[19] G. Kresse and J. Hafner, Phys. Rev. B **47**, 558 (1993); **49**, 14251 (1994).

[20] G. Kresse and D. Joubert, Phys. Rev. B **59**, 1758 (1999).

[21] Y. Wang and J. P. Perdew, Phys. Rev. B **44**, 13 298 (1991).

[22] R. F. Zhang, S. Veprek, and A. S. Argon, Appl. Phys. Lett. **91**, 201914 (2007); Phys. Rev. B **77**, 172103 (2008).

[23] A. R. West, *Solid State Chemistry and its Applications* (John Wiley & Sons, Chicester, 1984).

[24] Because of limited space available in this Letter, and due to the fact that the calculations of all stress-strain curves and their analysis are much time consuming, we shall present all the details of the relaxed and minimum energy structures in the full length paper to follow.

[25] A. S. Argon, *Strengthening Mechanisms in Crystal Plasticity* (Oxford University Press, Oxford, 2008).

[26] V. Vitek, Philos. Mag. **18**, 773 (1968).

[27] C. T. Bodur, J. Chang, and A. S. Argon, J. Eur. Ceram. Soc. **25**, 1431 (2005).

[28] S. Hao (private communication) 2008. Notice, that the calculation of the decohesion strength in the work of Hao *et al.* has been done by keeping the relative positions of the atoms in the upper and lower TiN layers of the modeled slabs fixed [13]. Therefore, Hao *et al.* could not see the effect of the Friedel oscillations.

[29] S. Christiansen, M. Albrecht, P. Strunk, and S. Veprek, J. Vac. Sci. Technol. B **16**, 19 (1998).

[30] A. S. Argon and S. Yip, Philos. Mag. Lett. **86**, 713 (2006).